Continuous doping of a cuprate surface: Insights from in situ angle-resolved photoemission

Y.-G. Zhong, J.-Y. Guan, X. Shi, J. Zhao, Z.-C. Rao, C.-Y. Tang, H.-J. Liu, Z. Y. Weng, Z. Q. Wang, G. D. Gu, T. Qian, Y.-J. Sun, and H. Ding

Phys. Rev. B **98**, 140507 — Published 24 October 2018

DOI: 10.1103/PhysRevB.98.140507

Continuous doping of a cuprate surface: Insights from *in-situ* ARPES

Y. -G. Zhong[1, 2, †], J. -Y. Guan[1, 2, †], X. Shi[1, 2], J. Zhao[1, 2], Z. -C. Rao[1, 2], C. -Y. Tang[1, 2], H. -J. Liu[1, 2], Z. Y. Weng[3, 4], Z. Q. Wang[5], G. D. Gu[6], T. Qian[1, 4], Y. -J. Sun[1, 7, *], and H. Ding[1, 2, 4, 7, *]

[1] *Beijing National Laboratory for Condensed Matter Physics and Institute of Physics, Chinese Academy of Sciences, Beijing 100190, China*

[2] *School of Physics, University of Chinese Academy of Sciences, Beijing 100190, China*

[3] *Institute for Advanced Study, Tsinghua University, Beijing 100084, China*

[4] *Collaborative Innovation Center of Quantum Matter, Beijing 100190, China*

[5] *Department of Physics, Boston College, Chestnut Hill, MA 02467, USA*

[6] *Condensed Matter Physics and Materials Science Department, Brookhaven National Laboratory, Upton, NY 11973, USA*

[7] *CAS Center for Excellence in Topological Quantum Computation, University of Chinese Academy of Sciences, Beijing, 100190, China*

[†] These authors contributed to this work equally.

[*] Corresponding authors: dingh@iphy.ac.cn, yjsun@iphy.ac.cn

Abstract

We report a new technique of continuously doped surface of $Bi_2Sr_2CaCu_2O_{8+x}$ through ozone/vacuum annealing and a systematic measurement over the nearly whole superconducting dome on a same sample surface by *in-situ* angle-resolved photoemission spectroscopy. We find that the quasiparticle weight on the antinode is proportional to the doped carrier concentration x within the entire superconducting dome, while the nodal quasiparticle weight changes more mildly. More significantly, we discover that a d-wave pairing energy gap extracted from the nodal region scales well with the onset temperature of Nernst signal. These new findings suggest that the emergence of superconducting pairing is concomitant with the onset of free vortices.

The high-T_c cuprate superconductors distinguish themselves from the conventional BCS superconductors in that a small variation in the carrier doping can significantly change the superconducting transition temperature (T_c), giving rise to a superconducting dome and a similarly dome-shape Nernst temperature (T_ν) for the onset of superconducting vortices well above T_c [1-3]. In the so-called underdoped (UD) region, a pseudogap [4,5] with highly controversial origins emerges at a temperature much higher than T_c and T_ν, whereas the system appears to gradually approach a Fermi liquid in the overdoped (OD) region. Therefore, a systematic study of the properties [6-8] over the whole superconducting dome is critical for understanding the cuprates superconducting mechanism. However, in many families of cuprates, like $Bi_2Sr_2CaCu_2O_{8+x}$ (Bi2212), high-quality crystals can be only obtained within a narrow doping range. Moreover, surface cleaving, necessary for surface techniques such as angle-resolved photoemission spectroscopy (ARPES) and scanning tunneling spectroscopy (STS) which have studied Bi2212 extensively [2, 9], posses a serious problem for quantitative comparisons from sample to sample. There are previous endeavors to *in-situ* dope the surface of cuprates by potassium evaporating or gas absorption [10-12], however, these methods introduce disorders to the surface that can affect the measured quantities.

Realizing that the doping level in this material is solely controlled by the excess oxygen concentration, we develop a new method of ozone/vacuum annealing to continuously change the doping level of the surface layers, which are subsequently measured by *in-situ* ARPES [Figs. 1(a)-1(c)]. Through this technique, we are able to obtain precise quantities of energy gaps including the pseudogap and the coherent spectral weight over a wide range of doping, revealing important new physical insights for the cuprates. In this paper, we demonstrate that the quasiparticle weight is linearly proportional to the doped carrier concentration x at the antinode, while it changes much more slowly with doping at the node. By extracting the gap slope around the node region, we discover that the d-wave component of the quasiparticle energy gap is linearly proportional to the Nernst temperature T_ν over the entire superconducting dome, strongly suggesting that the emergence of superconducting pairing is accompanied by the onset of free vortices, with direct implications for the strong fluctuation of SC phase far beyond T_c.

The optimally doped Bi2212 single crystals were grown by the floating-zone technique. Heating samples in an ultrahigh vacuum and ozone atmosphere were referred as the vacuum

annealing and ozone annealing, respectively. A high-quality optimally doped single crystal cleaved in a vacuum better than 1×10^{-7} Torr, then degased in a MBE chamber to ensure a surface, and annealed at ~470°C in the ozone atmosphere with a partial pressure about 4×10^{-6} Torr for 15 minutes to obtain a highly overdoped surface. The doping level of the surface was then reduced by a series of vacuum annealing processes with increasing heating powers. After each annealing process, the sample was transferred *in-situ* to an ARPES chamber for measurements. Freshness of a sample surface can be regenerated through each annealing process, and a sample surface can be measured over one month without noticeable contaminations. The *in-situ* ARPES measurements were carried in an ARPES system with a Scienta R4000 analyzer and a Scienta VUV source. The He Iα resonant line (hυ= eV) was used, and the vacuum of the ARPES chamber was better than 3×10^{-11} Torr. The and angular resolution was set at ~ 5meV and 0.2°, respectively.

It is well established that the electronic structure of doped CuO_2 planes of Bi2212 exhibits two-dimensional Fermi surface (FS) sheets whose area relative to the Brillouin Zone area is equal to $(1+x)/2$, where x is the doped carrier concentration [13]. Therefore, a precise determination of FS area by high-resolution ARPES, after taking extra care of the super-lattice and shadow FSs [Fig. 1(c)] (Ref.14), will provide the value of carrier concentration on the surface. Figures 1(d)-1(g) illustrate an example of how we continuously changing the doping level and the corresponding FS contour on one surface. Here we list a few noticeable features of the FS evolution: 1. There is a continuous reduction of the spectral weight on the FS going from overdoped (OD) to underdoped (UD), especially around the antinodal region, which is mainly caused by increasing of the superconducting gap and emergence of the pseudogap in the UD region. 2. The bilayer splitting [15], clearly visible in the OD region, gradually vanishes in the UD region due to the incoherent c-axis tunneling between adjacent CuO_2 planes. 3. The shrinkage of the FS area can be clearly visualized by the synchronized movement of the main FS and super-lattice FSs along the nodal direction [Fig. 1(e)]. A simple fitting to the measured FS [14] yields the carrier concentration of the surface [Fig. 1(f)]. Remarkably, a wide doping range within a nearly full SC dome can be continuously tuned on a single Bi2212 surface [Fig. 1(g)]. Such a "Phase-Diagram-on-Surface" (PDS) method, not only extends the doping range beyond the conventional single crystal method, but also eliminates the uncontrolled influence to ARPES spectral weight due to different flatness of cleaved surfaces, thus enabling precise analysis

and comparison of important quantities over the phase diagram of the cuprates.

One of the important quantities is the quasiparticle spectral weight (Z), which has been studied extensively by ARPES [16,17]. Despite of intensive efforts, reliable quantitative results of the doping evolution of Z and its momentum dependence are difficult to obtain due to its sensitivity to the surface condition that varies from sample to sample. The new PDS method overcomes this problem. A coherent quasiparticle peak emerges in the superconducting state [Figs. 2(a) and 2(b)], especially around the antinodal region, whose spectral weight (Z_{AN}) is believed to be related to the superfluid density or the superconducting phase stiffness [18]. Previous ARPES studies [16,17] have indeed revealed that Z_{AN} is proportional to x below the optimal doping level. However, the behavior of Z_{AN} on the overdoped side is controversial, with initial reports of saturating [16] or decreasing [17] behaviors. Figures 2(a) and 2(c) reveal that Z_{AN} on the antinodal FS is linearly proportional to x within the entire superconducting dome. We note that a saturating behavior is observed for the coherent weight at the M point that is not on the FS [14]. In the meantime, the PDS method also enables a precise measurement of the nodal quasiparticle weight (Z_N) that is known to be highly sensitive to the surface flatness. It is clear from Figs. 2(b) and 2(c) that the doping evolution of Z_N is much milder than that of Z_{AN}: it stays almost constant for a wide region on both sides of the optimal doping level, and decreases in the more underdoped region, possibly due to the appearance of Coulomb gap or other incoherent processes with heavy underdoping [19].

Another important quantity that can be systematically studied by the PDS method is the quasiparticle energy gap in the one-electron spectral function, which is a manifestation of both the superconducting gap and the possible pseudogap [4-6]. Since sharp quasiparticle peaks can be observed in the superconducting state at a low temperature, their peak position can be used as a good measure of the energy gap. The symmetrized peaks [20] remove the effect of the Fermi-Dirac function and thus give more precise values of the energy gap along the FS. We summarize the momentum dependence of the energy gap over a wide doping range ($0.07 \leq x \leq 0.24$) in Figs. 3(a)-3(f). In the OD region, e.g., $x = 0.24$ and 0.21, the momentum dependence of the energy gap follows the $\cos k_x$-$\cos k_y$ function nicely, reflecting the nature of a single d-wave pairing gap in this region. However, starting from $x = 0.18$, the energy gap extracted from the quasiparticle position deviates upward from the simple d-wave

function, and the deviation increases as the doping decreases [21]. This is indicative of the opening of the pseudogap whose origin has been widely debated [22,23]. It has been pointed out that the underlying superconducting gap follows the d-wave line visibly near the nodal region and extrapolates to the antinodal region, namely it follows the gap slope (Δ_0) [7,8]. We adopt this method that linearly extrapolates the superconducting gap around the node to the antinode [14] for all the doping levels [lower panels in Figs. 3(a)-3(f)]. If we regard the quasiparticle peak position as the superposition by quadrature of two energy gaps, as suggested previously [24,25] we can then decompose the total spectral gap (Δ_{tot}) into two gaps, $\Delta_{tot} = \sqrt{(\Delta_0^2 + \Delta_{PG}^2)}$, where Δ_0 and Δ_{PG} are the pairing gap and the pseudogap, respectively [Fig. 3(f)]. While the pairing gap, which is extrapolated from the nodal region, follows the d-wave function throughout the superconducting dome, the pseudogap opens up first at the antinodal region in the slightly OD region, and spreads toward the nodal region as the doping is reduced. We note that such a decomposition procedure is consistent with the observation of the pseudogap and the Fermi arc phenomena in the normal state above T_c in the UD regime.

A previous ARPES work [8] on single crystals of several doping levels suggested that this extrapolated energy gap is linearly proportional to T_c. However, a more precise study using our PDS method gives a qualitatively different result. Through a careful comparison between the gap at the antinode (Δ_{AN}) and the extrapolated gap (Δ_0), we find that the value of the extrapolated d-wave gap Δ_0 locates systematically in between the antinodal gap Δ_{AN} and the energy gap that would scale with T_c [Fig. 4(a)]. In the OD region, these two gaps and the T_c-scaled gap match very well. However, they start to diverge in the UD region, and the coupling strengths $2\Delta/k_BT_c$ obtained using these two gaps increase rapidly in the UD region [Fig. 4(b)], suggesting that neither T^* nor T_c are the thermal correspondence of the nodal d-wave gap in the quantum electronic state at low temperatures. Remarkably, if we replace T_c with the Nernst temperature T_ν [3], which was generally identified as a sign of Cooper pair formation, then $2\Delta_0/k_BT_\nu$ is nearly a constant over the whole SC dome [Fig. 4(b)], strongly indicating that the extrapolated gap Δ_0 represents a pairing energy gap associated with the formation of Cooper pairs, with a thermal correspondence to T_ν [Fig. 4(c)]. We note that the Nernst signal has been also interpreted as the contribution from the charge carrier (quasiparticle), not necessary from the superconducting fluctuation [26].

While we showed that the extrapolated nodal d-wave gap as the pairing energy scale

related to T_v, the origin of the pseudogap highlighted by the spectral gap around the antinode in the UD region remains an open question. Our measurements alone cannot rule out the scenario that the pseudogap stems from preformed pairs [25,27]. However, the divergent behavior of Δ_{PG} and Δ_0, naturally supports the notion that the pseudogap is due to competing order, such as the in the proposed scenarios of charge or bond order [28], valence bond glass [29], pair density wave [30], and loop current [31]. Recent experiments have indeed provided strong evidence for charge order in the UD region [28]. Although, we have not observed direct evidence for charge order here, but there is a residual spectral weight build up below the antinodal coherent peak, forming an "antinodal foot" in the UD region [Fig. 2(a) and Fig. S6 in Ref. 14]. It would be interesting in the future to study whether this antinodal foot is related to the charge order.

Our systematic measurements reveal a novel two-component coherent peak structure near the Fermi level over a wide range of doping. One has a d-wave-like gap Δ_0 near the nodal region with a much more slowly changing of coherent peak weight versus doping. But the characteristic energy Δ_0 itself is shown to scale with the Nernst temperature T_v, rather than T_c, by a ratio $2\Delta_0/K_BT_v \sim 6$ over the SC dome [Fig. 4(b)]. Here T_v can be interpreted as the onset of the pairing transition before pairing coherence is established, while the Nernst signal comes from the vortices of the local pairing order parameter above T_c. Namely the difference between T_v and T_c is due to the destruction of superconductivity by vortex fluctuations instead of vanishing Δ_0, and the true SC phase coherence is established at T_c. The region between T_v and T_c is anomalously large compared to conventional BCS superconductors, which is possibly a reflection of the energetically favorable vortex core states in the cuprates [1]. Note that the value of the ratio ~ 6 is comparable to the ratio of $2\Delta_0/K_BT_c$ between 4.6 and 5.6 [32] in the heaviest elemental superconductors such as Hg and Ir, which are in the strong coupling regime.

In contrast, an antinodal coherent peak with its spectral weight linearly proportional to *x* is observed to persist beyond the optimal doping. Previously, the antinodal weight has been argued to be related to the superfluid density in the SC state [16-18]. However, the superfluid density has been carefully measured in the overdoped regime of La-214 and found to decrease with the reduction of T_c [33]. Thus, our finding indicates that the antinodal spectral weight scales with the total carrier density *x* doped into the Mott insulating parent state over

the entire superconducting compositions. In the underdoped to optimally doped regions, they condense into the superfluid, whereas a significant portion may fail to condense in the overdoped region in sharp contrast to the BCS theory. It remains to be seen whether theories of doped Mott insulators [1,34] may account for the present ARPES observations.

Note added in proof. These papers are pertinent to the issues discussed in Supplemental Materials (Refs. 15-16 and Refs. 36-42).

References:

[1] P. A. Lee, N. Nagaosa, and X.-G. Wen, *Doping a Mott insulator: Physics of high-temperature superconductivity,* Reviews of modern physics **78**, 17 (2006).

[2] A. Damascelli, Z. Hussain, and Z.-X. Shen, *Angle-resolved photoemission studies of the cuprate superconductors,* Reviews of modern physics **75**, 473 (2003).

[3] Y. Wang, L. Li, and N. Ong, *Nernst effect in high-T_c superconductors,* Physical Review B **73**, 024510 (2006).

[4] H. Ding, T. Yokoya, J. Campuzano, T. Takahashi, M. Randeria, M. Norman, T. Mochiku, K. Kadowaki, and J. Giapintzakis, *Spectroscopic evidence for a pseudogap in the normal state of underdoped high-T_c superconductors,* Nature **382**, 51 (1996).

[5] A. Loeser, Z.-X. Shen, D. Dessau, D. Marshall, C. Park, P. Fournier, and A. Kapitulnik, *Excitation gap in the normal state of underdoped $Bi_2Sr_2CaCu_2O_{8+\delta}$,* Science **273**, 325 (1996).

[6] M. Hashimoto, I. M. Vishik, R.-H. He, T. P. Devereaux, and Z.-X. Shen, *Energy gaps in high-transition-temperature cuprate superconductors,* Nature Physics **10**, 483 (2014).

[7] I. Vishik, M. Hashimoto, R.-H. He, W.-S. Lee, F. Schmitt, D. Lu, R. Moore, C. Zhang, W. Meevasana, and T. Sasagawa, *Phase competition in trisected superconducting dome,* Proceedings of the National Academy of Sciences **109**, 18332 (2012).

[8] H. Anzai, A. Ino, M. Arita, H. Namatame, M. Taniguchi, M. Ishikado, K. Fujita, S. Ishida, and S. Uchida, *Relation between the nodal and antinodal gap and critical temperature in superconducting Bi2212,* Nature communications **4**, 1815 (2013).

[9] Ø. Fischer, M. Kugler, I. Maggio-Aprile, C. Berthod, and C. Renner, *Scanning tunneling spectroscopy of high-temperature superconductors,* Reviews of Modern Physics **79**, 353 (2007).

[10] M. Hossain, J. Mottershead, D. Fournier, A. Bostwick, J. McChesney, E. Rotenberg, R. Liang, W. Hardy, G. Sawatzky, and I. Elfimov, *In situ doping control of the surface of high-temperature superconductors,* Nature physics **4**, 527 (2008).

[11] Y. Zhang, C. Hu, Y. Hu, L. Zhao, Y. Ding, X. Sun, A. Liang, Y. Zhang, S. He, and D. Liu, *In situ carrier tuning in high temperature superconductor $Bi_2Sr_2CaCu_2O_{8+\delta}$ by potassium deposition,* Science bulletin **61**, 1037 (2016).

[12] A. Kaminski, S. Rosenkranz, H. Fretwell, M. Norman, M. Randeria, J. Campuzano, J. Park, Z. Li, and H. Raffy, *Change of Fermi-surface topology in $Bi_2Sr_2CaCu_2O_{8+\delta}$ with doping,* Physical Review B **73**, 174511 (2006).

[13] H. Ding, M. Norman, T. Yokoya, T. Takeuchi, M. Randeria, J. Campuzano, T. Takahashi, T. Mochiku, and K. Kadowaki, *Evolution of the Fermi surface with carrier concentration in $Bi_2Sr_2CaCu_2O_{8+\delta}$,* Physical review letters **78**, 2628 (1997).

[14] See Supplemental Materials at [URL] for following details: the origins of superlattice and shadow Fermi surfaces, the fitting procedure of Fermi surface, extracting procedure of quasiparticale weight and gap slope around node, and the leading edge foot of the EDCs in the UD region.

[15] D. Feng, N. Armitage, D. Lu, A. Damascelli, J. Hu, P. Bogdanov, A. Lanzara, F. Ronning, K. Shen, and H. Eisaki, *Bilayer splitting in the electronic structure of heavily overdoped $Bi_2Sr_2CaCu_2O_{8+\delta}$,* Physical review letters **86**, 5550 (2001).

[16] H. Ding, J. Engelbrecht, Z. Wang, J. Campuzano, S.-C. Wang, H.-B. Yang, R. Rogan, T. Takahashi, K. Kadowaki, and D. Hinks, *Coherent quasiparticle weight and its connection to high-T c superconductivity from angle-resolved photoemission,* Physical review letters **87**, 227001 (2001).

[17] D. Feng, D. Lu, K. Shen, C. Kim, H. Eisaki, A. Damascelli, R. Yoshizaki, J.-i. Shimoyama, K. Kishio, and G. Gu, *Signature of superfluid density in the single-particle excitation spectrum of $Bi_2Sr_2CaCu_2O_{8+\delta}$,* Science **289**, 277 (2000).

[18] P. W. Anderson, *The resonating valence bond state in La_2CuO_4 and superconductivity,* Science **235**, 1196 (1987).

[19] Z.-H. Pan, P. Richard, Y.-M. Xu, M. Neupane, P. Bishay, A. Fedorov, H. Luo, L. Fang, H.-H. Wen, and Z. Wang, *Evolution of Fermi surface and normal-state gap in the chemically substituted cuprates $Bi_2Sr_{2-x}Bi_xCuO_{6+\delta}$,* Physical Review B **79**, 092507 (2009).

[20] M. Norman, H. Ding, M. Randeria, J. Campuzano, T. Yokoya, T. Takeuchi, T.

Takahashi, T. Mochiku, K. Kadowaki, and P. Guptasarma, *Destruction of the Fermi surface in underdoped high-T_c superconductors,* Nature **392**, 157 (1998).

[21] N. Zaki, H.-B. Yang, J. D. Rameau, P. D. Johnson, H. Claus, and D. G. Hinks, *Cuprate phase diagram and the influence of nanoscale inhomogeneities,* Physical Review B **96**, 195163 (2017).

[22] T. Timusk and B. Statt, *The pseudogap in high-temperature superconductors: an experimental survey,* Reports on Progress in Physics **62**, 61 (1999).

[23] S. Hüfner, M. Hossain, A. Damascelli, and G. Sawatzky, *Two gaps make a high-temperature superconductor?,* Reports on Progress in Physics **71**, 062501 (2008).

[24] M. Civelli, M. Capone, A. Georges, K. Haule, O. Parcollet, T. Stanescu, and G. Kotliar, *Nodal-antinodal dichotomy and the two gaps of a superconducting doped Mott insulator,* Physical review letters **100**, 046402 (2008).

[25] C.-C. Chien, Y. He, Q. Chen, and K. Levin, *Two-energy-gap preformed-pair scenario for cuprate superconductors: implications for angle-resolved photoemission spectroscopy,* Physical Review B **79**, 214527 (2009).

[26] Cyr-Choinière, O., R. Daou, F. Laliberté, C. Collignon, S. Badoux, D. LeBoeuf, J. Chang et al. *Pseudogap temperature* T^* *of cuprate superconductors from the Nernst effect*. Physical Review B **97**, 064502 (2018).

[27] R. Boyack, Q. Chen, A. Varlamov, and K. Levin, *Cuprate diamagnetism in the presence of a pseudogap: Beyond the standard fluctuation formalism,* Physical Review B **97**, 064503 (2018).

[28] R. Comin and A. Damascelli, *Resonant x-ray scattering studies of charge order in cuprates,* Annual Review of Condensed Matter Physics **7**, 369 (2016).

[29] K.-Y. Yang, T. Rice, and F.-C. Zhang, *Phenomenological theory of the pseudogap state,* Physical Review B **73**, 174501 (2006).

[30] A. Melikyan and Z. Tešanović, *Model of phase fluctuations in a lattice d-wave superconductor: Application to the Cooper-pair charge-density wave in underdoped cuprates,* Physical Review B **71**, 214511 (2005).

[31] C. Varma, *Non-Fermi-liquid states and pairing instability of a general model of copper oxide metals,* Physical Review B **55**, 14554 (1997).

[32] B. Mitrović, H. Zarate, and J. Carbotte, *The ratio $2\Delta_0/k_BT_c$ within Eliashberg theory,* Physical Review B **29**, 184 (1984).

[33] I. Božović, X. He, J. Wu, and A. Bollinger, *Dependence of the critical temperature in*

overdoped copper oxides on superfluid density, Nature **536**, 309 (2016).

[34] Z.-Y. Weng, *Mott physics, sign structure, ground state wavefunction, and high-T_c superconductivity,* Frontiers of Physics **6**, 370 (2011).

[35] M. Presland, J. Tallon, R. Buckley, R. Liu, and N. Flower, *General trends in oxygen stoichiometry effects on T_c in Bi and Tl superconductors,* Physica C: Superconductivity **176**, 95 (1991).

[36] Ding, H., et al. Electronic Excitations in $Bi_2Sr_2CaCu_2O_8$: Fermi Surface, Dispersion, and Absence of Bilayer Splitting. *Phys. Rev. Lett.* **76**, 1533(1996). □

[37] Aebi, P., et al. Complete Fermi surface mapping of Bi-cuprates. *Journal of Physics and Chemistry of Solids* **56**, 1845-1847 (1995). □

[38] Saini, N. L., et al. Topology of the pseudogap and shadow bands in $Bi_2Sr_2CaCu_2O_{8+\delta}$ at optimum doping. *Phys. Rev. Lett.* **79**, 3467 (1997). □

[39] Aebi, Philipp, et al. Complete Fermi surface mapping of $Bi_2Sr_2CaCu_2O_{8+x}$ (001): Coexistence of short range antiferromagnetic correlations and metallicity in the same phase. *Physical Review Letters* **72**, 2757-2760 (1994). □

[40] Markiewicz R.S., Sahrakorpi S., Lindroos M., et al. One-band tight-binding model parametrization of the high-Tc cuprates including the effect of kz dispersion. Phys. Rev. B **72**, 054519 (2005) □

[41] Kaminski, A., et al. Quasiparticles in the superconducting state of $Bi_2Sr_2CaCu_2O_{8+\delta}$. *Phys. Rev. Lett.* **84**, 1788 (2000). □

[42] Mesot, J. et al. Superconducting gap anisotropy and quasiparticle interactions: a doping dependent photoemission study. *Phys. Rev. Lett*. **83**, 840–843 (1999).□

Acknowledgements:

We thank J. -J. Li, W. -Y. Liu, R. -T. Wang, J. -Q. Lin, F. -Z. Yang and S. -F. Wu for technique assistance and thank Q. J. Chen, K. Levin, J. X. Li, M. Randeria, F. C. Zhang for useful discussions. This work at IOP is supported by the grants from the Ministry of Science and Technology of China (2016YFA0401000, 2016YFA0300600, 2015CB921300, 2015CB921000), the Natural Science Foundation of China (11227903, 11574371, 11622435, 11474340), the Chinese Academy of Sciences (XDB07000000, XDPB08-1, QYZDB-SSW-SLH043), and the Beijing Municipal Science and Technology Commission (Z171100002017018). Z. Q. Wang is supported by the U.S. Department of Energy, Basic Energy Sciences Grant No. DE-FG02-99ER45747. G. D. Gu is supported by the office of BES, Division of Materials Science and Engineering, U.S. DOE, under contract Nos. de-sc0012704.

Author contributions:

Y-G. Z. carried out the ARPES experiments with contributions from X. S., J. Z., Z-C. R., C-Y. T., H-J. L., and T. Q.; J-Y. G. carried out the ozone annealing; Y-G. Z. carried out the vacuum annealing; G. D. G. synthesized the single crystals; Y-G. Z. and H. D. preformed the data analysis, figure development and wrote the paper with contributions from Z. Y. W., Z. Q. W., Y-J. S., and J-Y. G.; Y-J. S. and H. D. supervised the project. All authors discussed the results and interpretation.

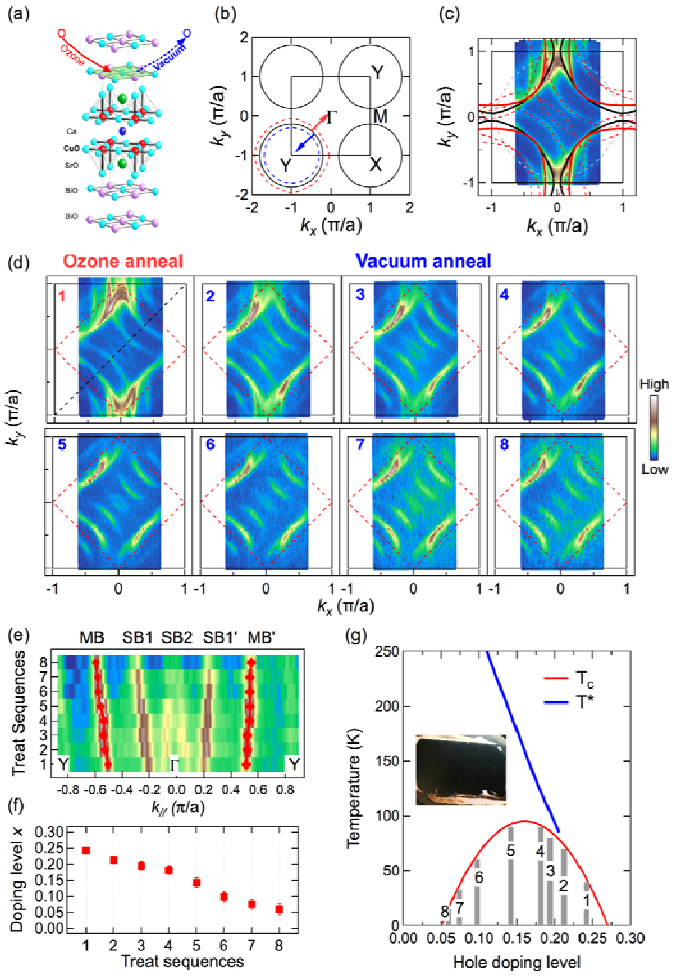

FIG. 1. (color online) (a) Crystal structure of Bi2212, and the schematic of ozone annealing (red arrows) and vacuum annealing (blue arrows) surface treatments. (b) The schematic FS of Bi2212 after ozone (red) and vacuum annealing (blue). (c) The FS of the OD one with considerations of super-lattice FS (red dash line) and shadow FS (gray dash line). The bold black and red lines are the fitting results corresponding to the antibonding and bonding FS, respectively. Those FSs are acquired at 30K with integrating ± 10meV around E_F. (d) The FS evolution with surface treat sequences: ozone annealing (panel 1), and a series of vacuum annealing (panels 2-8). (e) Image plot of the integrated intensity in the vicinity of E_F along the Γ-Y direction for each panel in (d), showing two main bands (MB, MB'), two 1st super-lattice bands (SB1, SB1'), and 2nd super-lattice bands (SB2). (f) The extracted doping level of each sequence. (g) The phase diagram of Bi2212: the red line is calculated with an empirical formula [35], the blue line is extracted from the antinodal gap closed temperature, the gray bars are the doping level for each sequence obtained in (f), and the insert picture is the one taken on the cleaved surface of this sample.

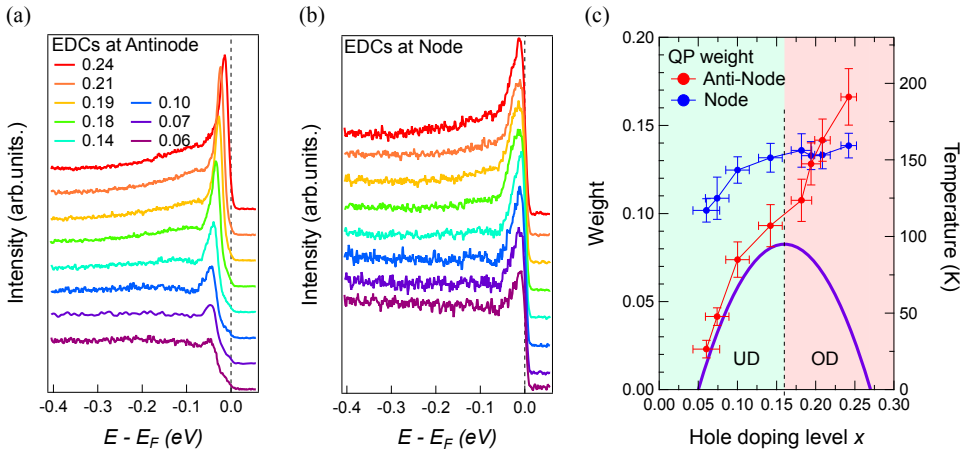

FIG. 2. (color online) (a) Antinodal EDCs at k_F evolution with doping. (b) Nodal EDCs at k_F evolution with doping measured on the same sample at 10K. (c) The extracting quasiparticle weight of the node and the antinode. The T_c line is plotted with the violet color.

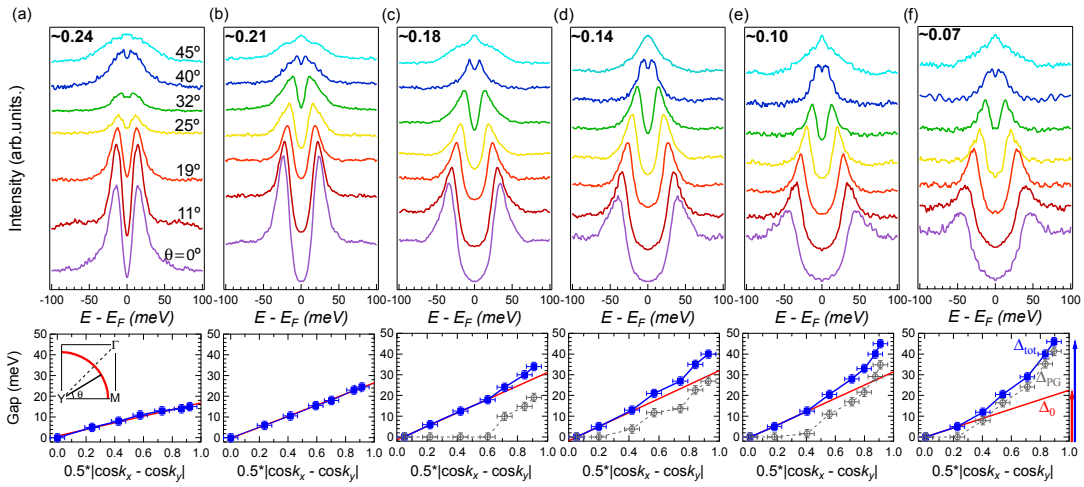

FIG. 3. (color online) (a-f) Upper panels display the symmetrized EDCs along the FS of six different doping levels. All data are measured on a same sample and a same temperature of ~10K. The corresponding momentum positions are indicated in a schematic diagram of FS in the inset of the lower panel of (a). Lower panels display the spectral gap along the FS (plotted against $0.5*|\cos k_x-\cos k_y|$) for different doping levels. The blue marked one is the total spectral gap, which is determined from the peak position of symmetrized EDCs, the red line is the corresponding d-wave gap function (details see SI) for each doping, and the gray marked one is the pseudogap obtained as describe in the text.

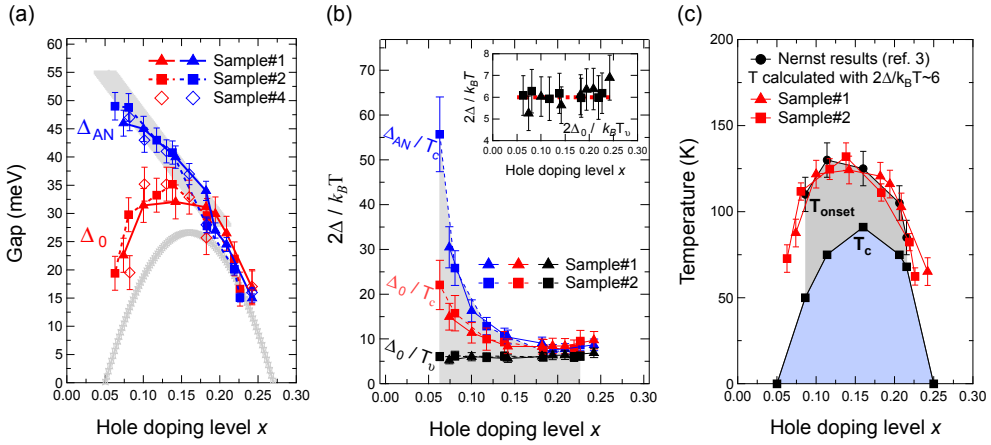

FIG. 4. (color online) (a) Doping dependence of the antinode gap Δ_{AN} and d-wave gap slope Δ_0. The red symbols are Δ_0, the blue ones Δ_{AN}, and the gray ones the T_c-scaled gap, with three different symbols (solid square, triangle and spaced rhombus) for three independent samples. (b) Doping dependence of $2\Delta/k_BT_c$. The blue symbols are $2\Delta_{AN}/k_BT_c$, the red ones $2\Delta_0/k_BT_c$, the black ones $2\Delta_0/k_BT_v$. The insert is a zoom-in plot to highlight the constant ratio of $2\Delta_0/k_BT_v$. The Nernst temperatures of the doping levels that are not included in Ref. 3 are estimated from a polynomial fitting to the data in Ref. 3. (c) A phase diagram of Bi2212. The red symbols are the pairing temperatures obtained from the constant ratio with Δ_0, the black dots the onset temperatures of the Nernst signal from ref. 3, black square ones the superconducting transition temperatures.